Optimal Energy Management and Techno-economic Analysis in Microgrid with Hybrid Renewable Energy Sources

Vallem V. V. S. N. Murty and Ashwani Kumar

***Abstract*—Microgrids with hybrid renewable energy sources are increasing and it is a promising solution to electrify remote areas where distribution network expansion is not feasible or not economical. Standalone microgrids with environment-friendly hybrid energy sources is a cost-effective solution that ensures system reliability and energy security. This paper determines the optimal capacity, energy dispatching and techno-economic benefits of standalone microgrid in remote area in Tamilnadu, India. Microgrids with hybrid energy sources comprising photovoltaic (PV), wind turbine (WT), battery energy storage system (BESS) and diesel generator (DG) are considered in this paper. Various case studies are implemented with hybrid energy sources and for each case study a comparative analysis of techno-economic benefits is demonstrated. Eight different configurations of hybrid energy sources are modeled with renewable fractions of 50%, 60%, 65%, and 100%, respectively. The optimization analysis is carried out using Hybrid Optimization Model for Electric Renewable (HOMER) software. Impact of demand response is also demonstrated on energy dispatching and techno-economic benefits. Simulation results are obtained for the optimal capacity of PV, WT, DG, converter, and BESS, charging/discharging pattern, state of charge (SOC), net present cost (NPC), cost of energy (COE), initial cost, operation cost, fuel cost, greenhouse gas emission penalty and payback period considering seasonal load variation. It is observed that PV+BESS is the most economical configuration. COE in standalone microgrid is higher than the conventional grid price. The results show that CO_2 emissions in hybrid PV+WT+DG+BESS are reduced by about 68% compared with the traditional isolated distribution system with DG.**

***Index Terms*—Microgrid, photovoltaic, wind turbine, diesel generator, battery energy storage system, greenhouse gas emissions, cost of energy.**

NOMENCLATURE

α, β	Parameters of Beta distribution
α_p	Temperature coefficient of power
η_{mp}	Efficiency of photovoltaic (PV) array at maximum power point
η_{Conv}	Efficiency of converter
η_{ch}	Charging efficiency
η_{dch}	Discharging efficiency
η_{WT}	Efficiency of wind turbine (WT)
$\mu_{P_{L,i}}, \mu_{Q_{L,i}}$	Means of active and reactive power
μ, σ	Mean and standard deviations of solar irradiation
σ_1	Battery self-discharging rate
$\sigma_{P_{L,i}}, \sigma_{Q_{L,i}}$	Standard deviations of power demand
$\rho(i)$	Spot electricity price at the i^{th} hour
$\rho_o(i)$	Initial electricity price at the i^{th} hour
Δd, Δp	Change in demand and price
$A(i)$	Amount of the incentive at the i^{th} hour
c	Weibull scale factor
$C_{ann,total}$	Total annualized cost
$C_{PV}, C_{WT}, C_{DG}, C_{BESS}, C_{Conv}$	Sum of present value of capital cost, operation and maintenance cost, replacement cost and fuel cost of PV, WT, DG, BESS, power converter during the project life time
CRF	Capital recovery factor
COE	Cost of energy
d_o, p_o	Initial demand and price
$d(i)$	Modified load demand due to DR at the i^{th} hour
$d_o(i)$	Initial load demand at the i^{th} hour
$D_{unmet,t}$	Total unmet energy demand
D_t	Total energy demand
$E_{ch}(t)$	Battery charging energy
$E_{dch}(t)$	Battery discharging energy
E_{served}	Total electrical load served
E	Price elasticity of demand
$E(i,i)$	Self-elasticity
$E(i,j)$	Cross elasticity
f	Inflation rate
f_{PV}	PV derating factor
$f_b(s)$	Beta distribution function of s

Manuscript received: April 30, 2020; accepted: August 20, 2020. Date of CrossCheck: August 20, 2020. Date of online publication: September 18, 2020.

V. V. V. S. N. Murty (corresponding author) and A. Kumar are with the Electrical Engineering Department, National Institute of Technology, Kurukshetra, Haryana, India (e-mail: murty209@gmail.com; ashwani.k.sharma@nitkkr.ac.in).

DOI: 10.35833/MPCE.2020.000273

$f(v)$	Weibull distribution function
$\overline{G}_T$	Solar radiation on PV array
$\overline{G}_{T,STC}$	Solar radiation at standard test conditions
$G_{T,NOCT}$	Solar radiation at which nominal operation PV cell temperature is defined
i	Actual rate of interest
i'	Discount rate of interest
INV_{cap}	Rating of inverter
k	Weibull shape factor
L_{ind}	Total inductive load
L_0	Total non-inductive load
N	Project life time
NPC	Net present cost
$pen(i)$	Penalty of DR program at the i^{th} hour
P_{PV}	Power output of PV array
P_{PV}^r	Rated capacity of PV array
P_{WT}	Power output of WT
P_{WT}^r	Rated power output of WT
P_{ch}	Charging power of battery energy storage system (BESS)
P_{dch}	Discharging power of BESS
P_{BESS}	Power output of BESS
P_{BESS}^r	Rated capacity of BESS
P_{DG}	The rated capacity of diesel generator (DG)
$P_{DG}^{\min}$	Minimum output power of DG
$P_{DG}^{\max}$	Maximum output power of DG
$P_{res,AC}$	Required operation reserve on AC bus
$P_{res,DC}$	Required operation reserve on DC bus
$P_{prime,AC}$	Average AC load
$P_{prime,DC}$	Average DC load
$\overline{P}_{prime,AC}$	Maximum AC load
$\overline{P}_{prime,DC}$	Maximum DC load
$P_{PV,avg}$	Average PV power output
$P_D(t)$	Load demand
$P_{DR}(t)$	Load demand after demand response (DR)
$P_g(t)$	Power import from grid
$P_n(v)$	WT power output function of wind speed
$P_{wind,AC}$	Average AC wind power output
$P_{L,i}, Q_{L,i}$	Active and reactive load demands
r_{load}	Operation reserve as percent of load
r_{wind}	Operation reserve as percentage of wind power output
r_{solar}	Operation reserve as percentage of PV power output
$r_{peak,load}$	Operation reserve as percent of peak load
s, s_r	Solar irradiance and its rated value
$SOC(t)$	Battery state of charge (SOC) at time t
T_c	PV cell temperature
$T_{c,STC}$	PV cell temperature at standard test conditions
T_a	Ambient temperature
$T_{c,NOCT}$	Nominal operation PV cell temperature
$T_{a,NOCT}$	Ambient temperature at which nominal operation PV cell temperature is defined
v, $\bar{v}$	Wind speed and its average value
v_{ci}, v_{co}	Cut-in and cut-out wind speeds

I. Introduction

EVEN though the expansion of generation, transmission and distribution systems are increasing day to day to cater growing electricity demand, as on today approximately 13% of world population has no access to electricity [1]. Integration of renewable energy sources with adequate energy storage devices is environment-friendly and provides diversification opportunities with additional revenue for remote areas. Optimally designed microgrid systems provide significant benefits of energy security, lower electricity rate, system reliability, integrating excess renewable power generation to microgrid, economic growth of rural areas by providing electricity to remote areas, and emission reduction. However, the optimal energy management in microgrid is a challenging task for microgrid operators (MGOs) with the optimal energy utilization of hybrid renewable energy sources and energy storage systems considering the uncertainty of load demand and renewable power generation.

A nano-grid was modeled in [2] using adaptive neuro-fuzzy inference system (ANFIS) considering photovoltaic (PV), wind turbine (WT) and battery energy storage devices to minimize the total cost. Simulation results were compared with Hybrid Optimization Model for Electric Renewable (HOMER) software and Hybrid Optimization by Genetic Algorithm (HOGA) software. It was concluded that better results were obtained using ANFIS compared with HOMER and HOGA in terms of total cost and excess power generated [2]. In [3], the integration of PV, WT and fuel cell in distribution system was reported using hybrid Nelder Mead-particle swarm optimization algorithm to minimize power loss. The location of distribution generation was obtained using voltage stability index. In [4], the model predictive control based energy management in microgrid was presented with WT and plug-in electric vehicles to minimize the operation cost. The load profile, WT power output and electricity price were estimated using seasonal autoregressive integrated moving average model. Also, the role of plug-in electric vehicles in demand response (DR) program was studied. In [5], the optimal energy scheduling problem was solved using alternating direction method of multipliers to minimize power fluctuations. In [6], the energy dispatching in grid connected microgrid with micro-turbine, fuel cell and battery energy storage devices was presented using mixed-integer quadratic programming to minimize operation cost. HOMER software was used in [7]-[19] to determine the optimal capacity of hybrid energy sources to quantify techno-economic benefits. Hybrid power system was simulated with hybrid energy sources in China [7], Nigeria [8], [13], Saudi Arabia [9],

[19], Iran [11], Turkey [14], and India [10], [17] to evaluate technical-economic benefits. The feasible solution was obtained based on the minimum cost of energy (COE) among different configurations of PV/battery energy storage system (BESS)/WT/fuel cell energy sources in Saudi Arabia [12]. The techno-commercial benefit of isolated grid with hybrid energy sources in Turkey was simulated using HOMER software [14]. It was concluded that the cost of energy in islanded grid mode is higher than the grid electricity. However, in future it is expected that COE is further reduced due to downward cost trend of BESSs. Further, it was stated that BESS technology was economical compared with fuel cell technology. The average cost of a typical microgrid with hybrid energy sources was estimated using HOMER software [15], [16].

However, associated cost components such as transformer cost, protection & measuring device cost, cable cost, battery degrading cost were not included. In [18], PV+BESS, WT+BESS, PV+WT+BESS, PV+fuel cell (FC), WT+FC and PV+WT+FC systems were simulated to investigate techno-economic benefits in Saudi Arabia. In [19], the PV+BESS based standalone microgrid system was simulated to demonstrate techno-economic benefits. In [20], the optimal capacity of WT+DG+BESS system was determined using stochastic optimization in standalone power system. In [21], the optimal capacity of PV/WT was determined using source sizing algorithm in grid-connected microgrid to minimize the total cost. Subsequently, the battery sizing algorithm was applied in the second stage to find the rating of BESS. In [22], the optimal size of BESS was determined in islanded microgrid with WT/PV/DG considering load growth scenario using the decomposition coordination algorithm. The techno-economic analysis of islanded microgrid with PV+WT+BESS was presented using genetic algorithm. In [23], the off-grid microgrid was modeled to provide power supply to telecommunication network at remote areas. In [24], the particle swarm optimization algorithm was adopted to determine the optimal capacity of PV/WT/DG/BESS/fuel cell in standalone minigrid in Australia. In [25], the optimal capacity of PV and BESS was determined using the particle swarm optimization for microgrid catering residential loads in Netherland and Texas. In [26], the energy dispatching and economic analysis in distribution system integrated with PV/WT/BESS were studied using the genetic algorithm. The economic energy dispatching strategy was formulated for microgrid with WT+BESS using the predictive optimization. In [27], the wind power and energy price were estimated using radial functional network. In [28], the optimal sizing of microgrid with hybrid PV+WT+BESS+DG was determined using the whale optimization algorithm (WOA), water cycle algorithm (WCA), moth-flame optimizer (MFO), and hybrid particle swarm-gravitational search algorithm to minimize the COE. In [29], the energy management in a community microgrid was presented considering the uncertainty of renewable energy sources, electricity price and load demand to minimize the total cost. In [30], the optimal size of BESS was determined using the mixed-integer programming for commercial applications integrated with PV system. In [31], the appropriate battery technology selection and sizing for microgrid expansion were solved using the mixed-integer linear programming.

It can be observed from the above literature survey that many researchers have focused on techno-economic analysis of microgrid without considering the impact of DR. Further, the potential benefit of DR program was not addressed in their analysis, which is essential for the effective operation of microgrid. The optimal energy dispatching with hybrid energy sources is a challenging task with consideration of load and generation uncertainties, which needs to be considered in the analysis for better system planning. Moreover, a comparative assessment of techno-economic benefits of various hybrid power systems considering DR program and seasonal load variation was not reported yet.

Based on the above research gaps, this paper investigates the optimal sizing of hybrid power system with PV/WT/DG/BESS, energy management, and techno-economic aspects of standalone microgrid. The HOMER software is used to model, simulate and optimize the hybrid power system to minimize COE and net present cost (NPC) subject to providing required operation reserve and reliability constraint of loss of power supply probability (LPSP) in conjunction with minimum excess energy production. In addition to optimal energy dispatching problem, a comparative analysis of techno-economic benefits is demonstrated for standalone microgrid with hybrid energy sources. Eight case studies are performed considering hourly varying seasonal load combination of residential and commercial loads throughout the year. The uncertainty of load demand is modeled using normal distribution function. Moreover, the impact of DR program on energy dispatching and techno-economic implications is also demonstrated. Simulation results are obtained for the optimal capacity of PV, WT, DG, BESS, charging/discharging pattern, state of charge (SOC), COE, NPC, initial cost, operation & maintenance (O&M) cost, fuel cost and payback period.

The estimated electricity consumption is 62039 kWh/year for the project site located far away from the main grid. Major activities of remote area communities include fishing and agriculture. The project site has abundant renewable energy sources of solar and wind. For accurate analysis, the real-time data of solar irradiation and wind velocity at the project site location are taken from National Renewable Energy Laboratory (NREL).

The rest of the paper is organized as follows. The modeling of hybrid power system is presented in Section II. The economic modeling is explained in Section III. The DR program is described in Section IV. Simulation results and discussions are presented in Section V. Finally, conclusions are drawn in Section VI.

II. Modeling of Hybrid Power System

The hybrid power system comprising PV/WT/BESS could be an economical solution to produce clean energy to match with time-varying realistic load demand and therefore the unmet energy demand shall be zero at any instant of time. The modeling of each source is explained in subsequent subsections.

A. PV

The output power of PV array is calculated as:

$$P_{PV}=P_{PV}^{r}f_{PV}\left(\frac{\overline{G}_{T}}{\overline{G}_{T,STC}}\right)\left[1+\alpha_{p}\left(T_{c}-T_{c,STC}\right)\right] \tag{1}$$

$$T_{c}=T_{a}\left(T_{c,NOCT}-T_{a,NOCT}\right)\frac{G_{T}}{G_{T,NOCT}}\left(1-\frac{\eta_{mp}}{0.9}\right) \tag{2}$$

The solar irradiation is modeled using the Beta distribution function, as expressed in (3)-(6).

$$f_{b}(s)=\frac{s^{\alpha-1}(1-s)^{\beta-1}}{\Gamma(\alpha)\Gamma(\beta)}\Gamma(\alpha+\beta) \tag{3}$$

$$\alpha=\mu\left[\frac{(1-\mu)\mu}{\sigma}-1\right] \tag{4}$$

$$\beta=(1-\mu)\left[\frac{(1-\mu)\mu}{\sigma}-1\right] \tag{5}$$

$$P_{PV}=\begin{cases}P_{PV}^{r}\dfrac{s}{s_{r}} & 0<s<s_{r}\\ P_{PV}^{r} & s_{r}<s\end{cases} \tag{6}$$

B. WT

The power output from WT is calculated as:

$$P_{WT}^{r}=\begin{cases}0 & v\le v_{ci}\\ P_{n}(v) & v_{ci}<v<v_{r}\\ 1 & v_{r}<v<v_{co}\\ 0 & v>v_{co}\end{cases} \tag{7}$$

$$P_{WT}=\eta_{WT}P_{WT}^{r} \tag{8}$$

The wind velocity is modeled using the Weibull distribution function as formulated in (9)-(11).

$$f(v)=\frac{k}{c}\left(\frac{v}{c}\right)^{k-1}\exp\left(\frac{-v}{c}\right)^{k}\quad 0\le v\le\infty \tag{9}$$

$$k=\left(\frac{\sigma}{\bar{v}}\right)^{-1.086} \tag{10}$$

$$c=\frac{\bar{v}}{\Gamma\left(1+\dfrac{1}{k}\right)} \tag{11}$$

C. BESS

The integration of renewable generation and electric vehicles to electric grid makes it more difficult to maintain energy balance and can result in large frequency deviations in the microgrid. Ancillary services provide supplementary reserve required to maintain the instantaneous and ongoing balance between sources and loads. BESSs can provide regulating reserve, a type of ancillary service, by modulating active power for frequency control, to reduce frequency deviations caused by sudden changes in renewable generation [32]. The rating of BESS is affected by battery configuration, back-up period, temperature, battery life time, depth of discharge, reserve power requirement and renewable energy sources, etc. The charging and discharging schedule of battery is expressed in (12).

$$P_{BESS}(t)=\begin{cases}P_{ch}(t) & P_{PV}(t)+P_{WT}(t)+P_{DG}(t)-P_{D}(t)\ge 0\\ P_{dch}(t) & P_{PV}(t)+P_{WT}(t)+P_{DG}(t)-P_{D}(t)<0\end{cases} \tag{12}$$

The charging and discharge power of BESS shall be less than the nominal capacity of BESS.

$$0\le P_{ch}(t)\le P_{BESS}^{r} \tag{13}$$

$$0\le P_{dch}(t)\le P_{BESS}^{r} \tag{14}$$

At a particular instant, a BESS can operate in one mode only, i.e., charging or discharging state. As specified in (12), the BESS operates in charging mode during surplus power generation and operates in discharging mode when the demand is more than the generation. The charging and discharging power of BESS is calculated as below.

1) Charging mode:

$$E_{ch}(t)=\left(\frac{P_{DG}(t)+P_{WT}(t)-P_{D}(t)}{\eta_{Conv}}+P_{PV}(t)\right)\Delta t\eta_{ch} \tag{15}$$

$$SOC(t)=(1-\sigma_{1})\cdot SOC(t-1)+E_{ch}(t) \tag{16}$$

2) Discharging mode:

$$E_{dch}(t)=\left(\frac{-P_{DG}(t)-P_{WT}(t)+P_{D}(t)}{\eta_{Conv}}-P_{PV}(t)\right)\Delta t\eta_{dch} \tag{17}$$

$$SOC(t)=(1-\sigma_{1})\cdot SOC(t-1)-E_{ch}(t) \tag{18}$$

D. Modeling of Power Converter

Converter is required in AC/DC hybrid power systems. The rating of inverter is determined using (19) [33].

$$INV_{cap}=3L_{ind}+L_{0} \tag{19}$$

E. Generator Capacity

The output power of diesel generator (DG) shall be within its upper and lower limits.

$$P_{DG}^{\min}\le P_{DG}\le P_{DG}^{\max} \tag{20}$$

F. Power Balance

The net power generation from PV, WT, DG and BESS shall be equal to the total load demand. Therefore, the unmet energy at any time shall be zero.

$$P_{D}(t)+P_{DR}(t)+P_{ch}(t)=P_{g}(t)+P_{DG}(t)+P_{WT}(t)+P_{PV}(t)+P_{ch}(t) \tag{21}$$

G. Reserve Power

Sudden disturbances of generation and load demands in the power system can initiate a steep fall or rise in the frequency of the power system, which can be detrimental to the power system operation if the disturbances are not cleared immediately. The corrective action shall be taken instantaneously to regulate frequency as per statutory limit by providing real power operation reserve which acts instantaneously with frequency change. The grid operators must have planned the adequate amount of reserve power capacity at strategic locations in the grid to ensure reliable power supply for 24×7 despite the intermittent nature of renewable power and the uncertainty of load demand.

$$P_{res,AC}=r_{load}P_{prime,AC}+r_{peak,load}\overline{P}_{prime,AC}+r_{wind}P_{wind,AC} \tag{22}$$

$$P_{res,DC} = r_{load} P_{prime,DC} + r_{peak,load} \overline{P}_{prime,DC} + r_{solar} P_{PV,avg} \quad (23)$$

H. LPSP

In case the load demand is more than the generation, a situation arises that the customer energy demand is not served completely, i.e., there is loss of power supply. The LPSP is a design indicator which measures the probability of unmet energy demand, as given in (24). The formula of the availability of power supply (APS) is given in (25).

$$LPSP = \frac{\sum_{t=1}^{T} D_{unmet,t}}{\sum_{t=1}^{T} D_t} \quad (24)$$

$$APS = 1 - LPSP \quad (25)$$

To ensure the reliability, the energy generated $P_{gen}(t)$ shall be greater than energy demand at any instant.

$$P_{gen}(t) > P_D(t) \quad (26)$$

I. Modeling of Load Uncertainty

The uncertainty of electricity demand is modeled using the normal distribution function [34] as given in (27) and (28).

$$f\left(P_{L,i}\right) = \frac{1}{\sigma_{P_{L,i}}\sqrt{2\pi}} \exp^{-\frac{\left(P_{L,i} - \mu_{P_{L,i}}\right)^2}{2\sigma^2_{P_{L,i}}}} \quad (27)$$

$$f\left(Q_{L,i}\right) = \frac{1}{\sigma_{Q_{L,i}}\sqrt{2\pi}} \exp^{-\frac{\left(Q_{L,i} - \mu_{Q_{L,i}}\right)^2}{2\sigma^2_{Q_{L,i}}}} \quad (28)$$

III. Economic Modeling

The HOMER software [35] optimizes various possible configurations and ranks each feasible configuration based on NPC. Capital, replacement, O&M, and fuel costs are included in the NPC calculation. The NPC is calculated using (29).

$$NPC = \frac{C_{ann,total}}{CRF(i,N)} \quad (29)$$

The $CRF(i,N)$ is determined by:

$$CRF(i,N) = \frac{i(1+i)^N}{i(1+i)^N - 1} \quad (30)$$

$$i = \frac{i' - f}{1+f} \quad (31)$$

The levelized COE is the ratio of the total annualized cost to the total electrical load served.

$$L_{COE} = \frac{C_{ann,total}}{E_{served}} \quad (32)$$

$$NPC = C_{PV} + C_{WT} + C_{DG} + C_{BESS} + C_{Conv} \quad (33)$$

The HOMER software determines the economical configuration of hybrid power system, capacity of each component and cash flow summary. The software simulates microgrid with all feasible combinations of hybrid energy sources and energy storage devices and determines the most economical configuration based on NPC and COE. Three major steps involved in the HOMER software are simulation, optimization and sensitivity analysis. A set of constraints of power balance, diesel power limits, reserve power requirement and grid power import/export limits shall be specified. During the optimization process, all possible hybrid power system configurations are optimized and the most viable configuration is selected based on the lowest NPC and COE. The sensitivity analysis is used to investigate the impact of sensitivity variables on optimization results. For example, the sensitivity analysis is useful to study the impact of fuel price, battery life time, type of storage, solar irradiation level and wind speed on the optimal system design.

The microgrid energy management (MGEM) involves the following main blocks of monitoring (load forecasting demand, renewable power generation, utility electricity price, etc.), controlling (distributed energy resource on/off control, switching of controllable loads, battery SOC, power import/export from grid), and optimization to achieve the minimum COE, maintain supply-demand balance and provide reliable power supply to all customers. The key issues of MGEM include the microgrid system configuration, coordination of hybrid energy sources, adequate energy storage capacity to ensure reliability, energy management and control. For effective MGEM, the bidirectional communication link is essential between grid controller and microgrid controller. The energy management module of central controller is responsible for the optimal energy dispatching in microgrids. The problem of MGEM involves finding the optimal unit commitment (UC) and optimal energy dispatching to achieve set objectives.

The polycrystalline type Huawei SUN2000 flat plate PV panel is considered in the simulation study. The rated capacity of the PV system is 40 kW. The operation temperature is 45 °C, the temperature coefficient of PV panel is −0.41, the efficiency of PV panel is 17.30% and the life time is set as 25 years. The capital and replacement cost of the PV system is considered as 900 $/kW and the O&M cost is 10 $/kW per year. The monthly average solar radiation and temperature are illustrated in Figs. 1 and 2. The WT of Bergey is considered in this paper. The capital and replacement cost of WT system is set as 15000 $/kW, the O&M cost is set as 75 $/kW per year and the life time is set as 20 years. The cut-in and cut-out speeds are taken as 3 m/s and 20 m/s, respectively. The rated capacity of WT is 10 kW and the hub height is 24 m. The DG of TD Power Systems (TDPS) is considered in the simulation study. The capital and replacement cost of DG is considered as 500 $/kW, the O&M cost is 0.03 $/kW per year and the fuel price is 1 $/L . The penalty rates for CO_2, CO, SO_2 and NO_x emissions are set at 0.03 $/kg, 0.03 $/kg, 2.18 $/kg and 9.26 $/kg, respectively. BESS of Trojan with nominal capacity of 72 kWh is taken in the simulation study. The nominal voltage is 60 V. The BESS comprises 10 batteries in 10 parallel strings. Therefore, the available nominal capacity of BESS is 720 kWh. The maximum charging and discharging currents of BESS are 250 A and 500 A, respectively. The capital and replacement cost of BESS is considered as 350 $/kW, the O&M cost is 10 $/kW per year and the life time is set as 20 years. The maximum capacity of DG is 60 kW and the minimum output is 20 kW. The BESS has a maximum charging and discharging power

of 50 kWh and a capacity of 100 kWh, respectively. In order to increase the life of the BESS, the minimum and maximum SOCs are set as 20% and 95%, respectively. The rated capacity of system converter is 30 kW. The limit on power import and export to the main grid is considered as 80 kW. The nominal discount rate as 8% and the inflation rate as 2% are considered in the simulation study for the project life time of 25 years.

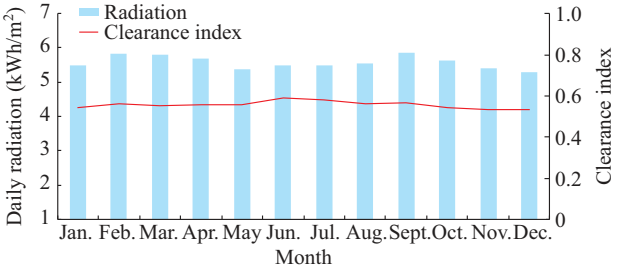

Fig. 1. Monthly profile of average solar radiation.

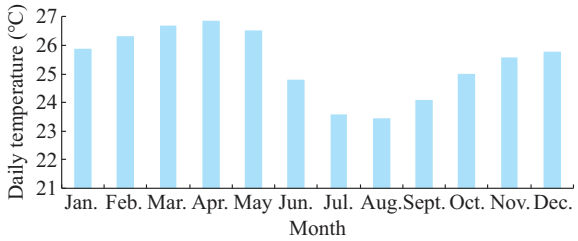

Fig. 2. Monthly profile of average temperature.

IV. Implementation of DR Programs

Demand-side participation is an important aspect for optimal energy scheduling at lower cost and higher security [36]. DR is one of the most popular methods of demand-side participation that encourages the customers to adjust their elastic loads in accordance with the operator's request or price signals. Usually, the elastic loads are classified into shiftable loads and curtailable loads. The benefits of DR for customers include cost savings and continuity of electricity. It also has benefits for MG operators such as cost savings, optimal operation, reduced use of costly generators, reduced purchase of expensive power from the main grid and load curve flattening. In general, DR programs are classified into two main categories of time-based rate (TBR) and incentive-based (IB) programs. In the TBR program, the motivation to change customer demand is related to the difference in electricity prices at different time, while in the IB program, incentive and penalty options are the motivation behind the change in customer demand.

A. Modeling of Demand Price Elasticity

The elasticity is defined as the load sensitivity with respect to the electricity price as expressed in (34) [37].

$$E=\frac{\Delta d/d_0}{\Delta p/p_0} \tag{34}$$

The elasticity is composed of two different coefficients namely self-elasticity and cross-elasticity. The self-elasticity is a measure of the load curtailment while the cross-elasticity is a measure of the load shifting. The self-elasticity is defined as the change in demand at a time instant i, due to change in price at the same time instant i as represented in (35). Since the change in price will have an inverse effect on the change in demand, self-elasticity $E(i,i)$ takes a negative value. The cross-elasticity is defined as the change in demand at time instant i due to change in price at some other time instants j as represented in (36). The cross-elasticity $E(i,j)$ is either positive or zero depending on whether the customer is willing to shift their load or not.

$$E(i,i)=\frac{\partial d(i)/d_o(i)}{\partial p(i)/p_o(i)}\le 0 \tag{35}$$

$$E(i,j)=\frac{\partial d(i)/d_o(i)}{\partial p(j)/p_o(i)}\ge 0 \tag{36}$$

The price elasticity matrix will be of the order 24×24 for 24 hours of a day as represented in (37). The diagonal elements of the price elasticity matrix represent self-elasticity coefficients and the off-diagonal elements represent cross-elasticity coefficients.

$$\begin{bmatrix}\frac{\Delta d(1)}{d_o(1)}\\ \frac{\Delta d(2)}{d_o(2)}\\ \vdots\\ \frac{\Delta d(24)}{d_o(24)}\end{bmatrix}=\begin{bmatrix}E(1,1) & E(1,2) & \cdots & E(1,24)\\ E(2,1) & E(2,2) & \cdots & E(2,24)\\ \vdots & \vdots & & \vdots\\ E(24,1) & E(24,2) & \cdots & E(24,24)\end{bmatrix}\begin{bmatrix}\frac{\Delta p(1)}{p_o(1)}\\ \frac{\Delta p(2)}{p_o(2)}\\ \vdots\\ \frac{\Delta p(24)}{p_o(24)}\end{bmatrix} \tag{37}$$

The electricity prices are assumed as 0.03 \$/kWh in flat rate, and 0.012 \$/kWh, 0.02 \$/kWh and 0.05 \$/kWh at valley, off-peak and peak periods, respectively. In this case, we assume electricity prices of 0.025 \$/kWh and 0.01 \$/kWh have the incentive and penalty rates, respectively. According to Table I, the load curve is divided into three different periods, namely valley period, off-peak period and peak period.

TABLE I
Self-elasticity and Cross-elasticity for 24 Hours

Period	Elasticity			Time period (hour)
	Valley	Off-peak	Peak	
Valley	–0.100	0.010	0.012	1-9
Off-peak	0.010	–0.100	0.016	10-18
Peak	0.012	0.016	–0.100	19-24

B. Load Control in TBR Program

In the TBR program, the customer load demand changes with respect to the electricity price signals. The modified load demand due to the implementation of TBR program is obtained from the following equation.

$$d(i)=d_o(i)\left(1+E(i)\frac{\rho(i)-\rho_o(i)}{\rho_o(i)}+\sum_{j=1,j\ne i}^{24}E(i,j)\frac{\rho(j)-\rho_o(j)}{\rho_o(j)}\right)\quad i=1,2,\ldots,24 \tag{38}$$

C. Load Control in IB Program

In the IB program, the changes in electricity usage is

based on incentive and penalty options in certain periods, such as peak periods. The modified load demand due to the implementation of IB program is obtained as:

$$d(i)=d_o(i)\left(1+E(i)\frac{\rho(i)-\rho_o(i)-A(i)+pen(i)}{\rho_o(i)}+\sum_{j=1,j\neq i}^{24}E(i,j)\frac{\rho(j)-\rho_o(j)-A(j)+pen(j)}{\rho_o(j)}\right) \quad (39)$$

V. Results and Discussions

The optimal energy management is a challenging task for MGOs with optimal utilization of hybrid energy sources and energy storage devices considering uncertain environment. This paper simulates the standalone microgrid with PV/WT/DG/BESS at remote village in Tamil Nadu, India using HOMER software to quantify techno-economic benefits. The optimal power system configuration is also determined based on the COE and annual NPC. The hybrid power system is modeled to cater the varying seasonal residential and commercial loads for the project site. In this paper, the hybrid power system is designed to provide the minimum requisite operation reserve to ensure the grid reliability. A comparative analysis of techno-economic and environment benefits is presented with different configurations of PV+BESS, WT+BESS, DG+BESS, PV+DG+BESS, WT+DG+BESS, PV+WT+BESS and PV+WT+DG+BESS with and without DR.

A. Without DR

As mentioned in the previous section, eight different configurations of hybrid power systems are optimized considering hourly variation of load, wind velocity, solar radiation and ambient temperature. The peak electricity demand occurs during evening hours (06:00-10:00 p.m.), which cannot be catered using PV or WT due to the non-availability of adequate solar or wind power output. Therefore, the hybrid power system comprising of PV/WT/BESS could be an economical solution to produce 24×7 clean energy to match with time-varying realistic load demand. In this way, the hybrid power system is able to cater both the base load and the flexible load. The optimal configuration of hybrid power system (PV+BESS) can deliver requisite power for 24×7 at a cost of 0.124 $/kWh. This provides a framework to promote hybrid power systems for electrifying remote areas. The comparative analysis of techno-economic benefits for various configurations is given in Tables II-V. The system configuration details for each configuration are given in Table II. Table II shows the optimal capacity of PV, WT, DG, BESS for each case study. The analysis has been carried out considering 100%, 65%, 60% and 50% of renewable energy contribution, respectively. From Table III, it can be observed that the levelized COE is low for PV+BESS (0.124 $/kWh) and high for WT+BESS (0.7273 $/kWh). The integration of DG has great influence on COE than BESS. The annual NPC is low for PV+BESS ($99427.02) and high for the microgrid with DG ($502348.3).

The annual energy production details of each configuration are given in the Table IV. The total annual load consumption of the system is 62039 kWh/year, which is met by PV power production of 44588 kWh/year, DG power production of 25789 kWh/year and WT power production of 2865 kWh/year in the PV+WT+DG+BESS configuration.

TABLE II
Simulation Results of Various Configurations

Configuration	Result of PV (kW)	Result of WT (kW)	Number of BESS	Result of DG (kW)	Result of converter (kW)
PV+WT+BESS+DG	25	10	10	5	17.5
PV+DG+BESS	17		300	5	26.0
WT+DG+BESS		70	50	7	30.3
PV+WT+BESS	40	10	43		22.0
PV+BESS	41		65		22.7
WT+BESS		200	377		31.0
DG+BESS			3	8	14.7
DG				23	

TABLE III
Economic Results of Various Configurations

Configuration	NPC ($)	COE ($/kWh)	Operation cost ($/year)
PV+WT+BESS+DG	199850.80	0.2492	11081.21
PV+DG +BESS	319414.80	0.3982	13700.61
WT+DG +BESS	424570.30	0.5296	21335.14
PV+WT+BESS	103661.70	0.1293	1635.06
PV+BESS	99427.02	0.1240	1758.84
WT+BESS	583120.80	0.7273	9893.38
DG+BESS	342131.30	0.4266	25224.18
DG	502348.30	0.6263	37969.26

TABLE IV
Annual Energy Production of Various Configurations

Configuration	Resource	Annual energy production (kWh/year)	Fraction (%)
PV+WT+DG+BESS	PV	44588	60.90
	WT	2865	3.91
	DG	25789	35.20
PV+DG+BESS	PV	30276	57.80
	DG	22088	42.20
WT+DG+BESS	WT	20058	28.80
	DG	49615	71.20
PV+WT+BESS	PV	71408	95.90
	WT	3072	4.12
PV+BESS	PV	73192	100.00
WT+BESS	WT	57309	100.00
DG+BESS	DG	67720	100.00
DG	DG	69259	100.00

It is observed from the simulation results that the total electricity demand is supplied by 64.8% renewable fraction and 32.2% non-renewable fraction in PV+WT+DG+BESS configuration. As specified in the Table II, the PV+WT+DG+BESS configuration consists of 25 kW PV, 10 kW WT, 5 kW DG set, 10 battery strings and 17.5 kW converter. The

cash flow summary of hybrid power systems is shown in Fig. 3. The hourly optimal power dispatching of the hybrid power system is illustrated in Fig. 4 to balance the electricity demand and power generation subject to the minimization of annual NPC. Among various feasible configurations, it is observed that the PV+BESS configuration is the most economical compared with other configurations considered in the simulation study.

TABLE V
SUMMARY OF OUTPUT POWER OF DIFFERENT ENERGY SOURCES

Source	Parameter	Value							
		DG	DG+BESS	WT+BESS	PV+BESS	PV+WT+BESS	WT+BESS+DG	PV+BESS+DG	PV+WT+DG+BESS
PV	Rated capacity (kW)				41	40		17	25
	Mean output (kW)				8.36	8.15		3.46	5.09
	Mean output (kWh/day)				201.0	196.0		82.9	122.0
	Capacity factor (%)				20.4	20.4		20.3	20.4
	Total production (kWh/year)				73192	71408		30276	44588
	Minimum output (kW)				0	0		0	0
	Maximum output (kW)				40.5	39.5		16.8	24.7
	PV penetration (%)				118.0	115.0		48.8	71.9
	Operation hours per year				4380	4380		4380	4380
	Levelized cost ($/kWh)				0.0446	0.0446		0.0447	0.0446
WT	Total rated capacity (kW)			200		10	70		10
	Mean output (kW)			6.540		0.351	2.290		0.327
	Capacity factor (%)			3.27		3.51	3.27		3.27
	Total production (kWh/year)			57309		3072	20058		2865
	Minimum output (kW)			0		0	0		0
	Maximum output (kW)			195.00		9.77	68.10		9.73
	Wind penetration (%)			92.4		4.95	32.3		4.62
	Operation hours per year			6041		6011	6041		6041
	Levelized cost ($/kWh)			0.476		0.444	0.476		0.476
DG	Operation hours per year	8760	8468				7681	6102	6615
	Number of starts per year	1	108				2	1	57
	Operation life (year)	1.71	1.77				1.95	2.46	2.27
	Capacity factor (%)	34.4	96.6				80.9	50.4	58.9
	Fixed generation cost ($/h)	2.220	0.771				0.674	0.482	0.482
	Marginal generation cost ($/kWh)	0.273	0.273				0.273	0.273	0.273
	Electrical production (kWh/year)	69259	67720				49615	22088	25789
	Mean electrical output (kW)	7.91	8.00				6.46	3.62	3.90
	Minimum electrical output (kW)	5.75	2.00				1.75	1.25	1.25
	Maximum electrical output (kW)	23	8				7	5	5
BESS	Number of batteries		3	377	65	43	50	300	10
	Number of string size		1	1	1	1	1	1	1
	Number of strings in parallel		3	377	65	43	50	300	10
	Bus voltage (V)		60	60	60	60	60	60	60
	Autonomy (hour)		30.5	3066	661	437	508	3049	102
	Storage wear cost ($/kWh)		0	0	0	0	0	0	0
	Nominal capacity (kWh)		216	27144	4680	3096	3600	21600	720
	Usable nominal capacity (kWh)		216	21715	4680	3096	3600	21600	720
	Life time throughput (kWh)		269473	854837	811685	763374	427787	726111	575210
	Expected life (year)		20	20	20	20	20	20	20
	Average energy cost ($/kWh)		0.397	0	0	0	0.248	0.105	0.131
	Energy input (kWh/year)		15721	24792	42325	41392	23380	18684	33387
	Energy output (kWh/year)		11433	36268	34437	32387	18149	30806	24404
	Storage depletion (kWh/year)		134	21705	4670	3046	1551	20452	431
	Loss (kWh/year)		4422	10229	12558	12051	6781	8329	9414
	Annual throughput (kWh/year)		13474	42742	40584	38169	21389	36306	28761

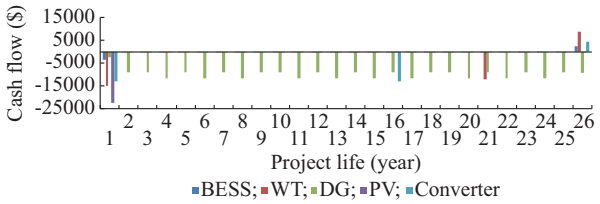

Fig. 3. Cash flow summary of PV+WT+DG+BESS configuration.

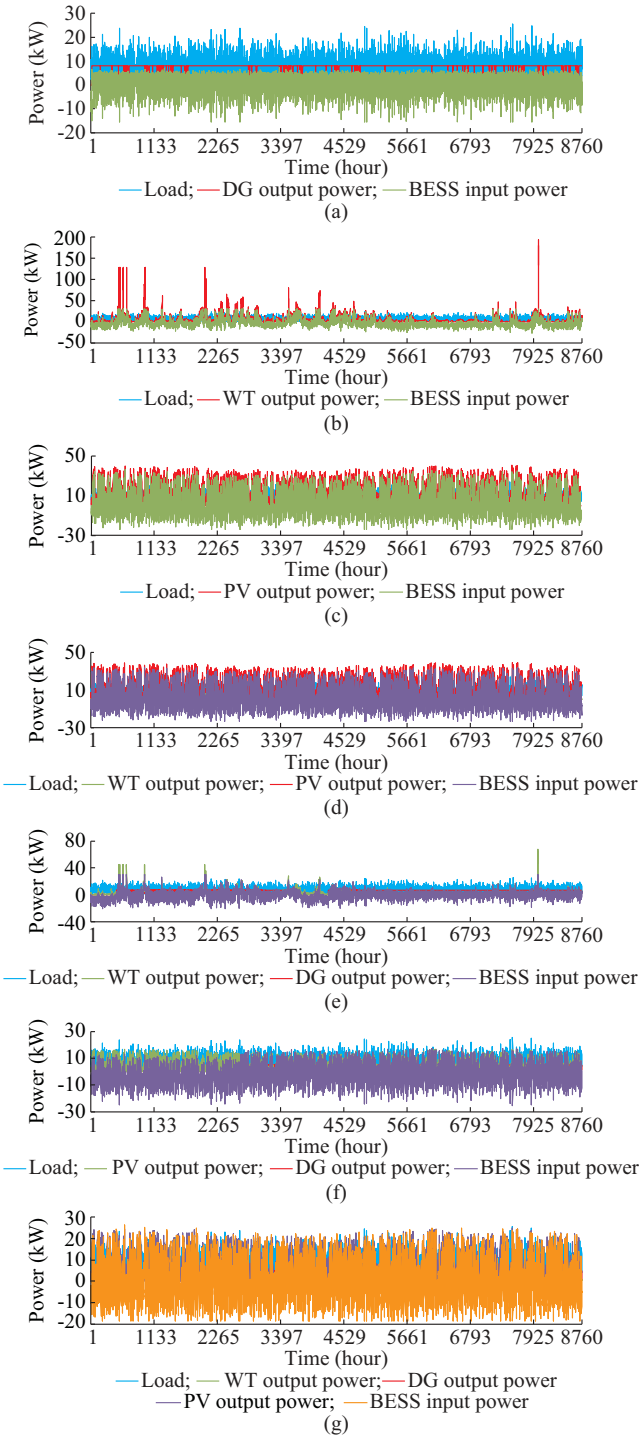

Fig. 4. Optimal power dispatching in microgrid with various configurations. (a) DG+BESS. (b) WT+BESS. (c) PV+BESS. (d) PV+WT+BESS. (e) WT+DG+BESS. (f) PV+DG+BESS. (g) PV+WT+DG+BESS.

The COEs of the hybrid power systems are 0.124 $/kWh, 0.2492 $/kWh, 0.3982 $/kWh, and 0.5292$/kWh with renewable fractions of 100%, 65%, 58%, and 28%, respectively. Similarly, the NPCs of the hybrid power systems are $99427, $199850, $319414, and $424570 with renewable fractions of 100%, 65%, 58%, and 28%, respectively. It is observed that COEs and NPCs are inversely varying with renewable fractions. It is obtained from the cost summary of the hybrid power systems that the capital cost of PV+WT+DG+BES configuration is lower compared with other systems. It should also be noted that the payback periods of PV+WT+DG+BESS, PV+DG+BESS, WT+DG+BESS, PV+WT+BESS, PV+BESS configurations are 0.34 year, 0.54 year, 0.72 year, 0.177 year and 0.17 year, respectively, compared with WT+BESS configuration.

Table VI and Table VII demonstrate the reduction in greenhouse gas emissions in microgrid with renewable energy sources compared with conventional isolated distribution system with DGs. In Table VI, UHC stands for unburned hydrocarbon and PM stands for particulate matter. The PV+WT+DG+BESS configuration reduces CO and CO_2 emissions by 68.1% per year compared with off-grid microgrid system operating with DG. After implementing the DR program, CO and CO_2 emissions are reduced by 67.7% per year as compared with the islanded microgrid system operating with DG alone.

TABLE VI
GREENHOUSE GAS EMISSIONS

Configuration	Emission (kg/year)					
	CO_2	CO	UHC	PM	SO_2	NO_x
DG	66904	418	18.40	2.500	164.0	393
DG+BESS	54250	339	14.90	2.030	133.0	318
WT+BESS+DG	40104	250	11.00	1.500	98.2	235
PV+BESS+DG	18421	115	5.07	0.690	45.1	108
PV+WT+DG+BESS	21288	133	5.85	0.797	52.1	125

TABLE VII
GREENHOUSE GAS EMISSION SUMMARY WITH DR

Configuration	Emission (kg/year)					
	CO_2	CO	UHC	PM	SO_2	NO_x
DG	61086	381	16.80	2.280	149.7	358.8
DG+BESS	47468	296	13.00	1.770	116.3	278.2
WT+BESS+DG	37833	299	13.20	1.790	117.0	281.0
PV+BESS+DG	26051	163	7.16	0.975	63.8	153.0
PV+WT+DG+BESS	19732	123	5.43	0.739	48.3	116.0

B. Simulation Results Considering Reserve Power

The brief summary of simulation results is presented considering the reserve power with BESS to ensure microgrid resilience during unexpected outages. The optimal size of PV+BESS configuration is determined for cost savings and enhanced resilience of the system. In this paper, the system is optimized to minimize the life cycle COE without considering resilience factor and then the system is re-optimized considering resilience. Simulation results are obtained with

PV+BESS configuration to sustain the critical load and ensure the grid resilience. The system is designed to sustain the 50% critical load during the specified outage period for 48 hours. The hourly power dispatching results considering resilience are shown in Fig. 5. The hybrid power system includes PV system with rated power of 449 kW and BESS with rated power and capacity of 136 kW and 746 kWh. Detailed simulation results for resilience is demonstrated in Table VIII, where model 1 is business as usual; model 2 is resilience model; model 3 is financial model; and CAPEX stands for capital expense. Outages are simulated starting at every hour of the year and the amount of time that the system can sustain the critical load during each outage is calculated, as shown in Fig. 6. From the simulation results, it is observed that the capacity of PV+BESS configuration increases when the resilience is considered.

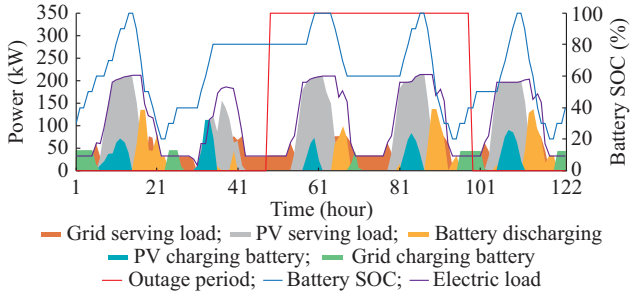

Fig. 5. Hourly power dispatching results considering resilience.

TABLE VIII
COMPARISON OF SIMULATION RESULTS CONSIDERING RESILIENCE

Parameter	Mode 1	Mode 2	Mode 3
Survived in specified outage	No	Yes	No
Average outage time (hour)	0	1020	10
Minimum outage time (hour)	0	2	0
Maximum outage time (hour)	0	4052	63
PV size (kW)	0	449	366
Annualized PV energy production (kWh)	0	716554	584728
Battery power (kW)	0	136	75
Battery capacity (kWh)	0	746	231
NetCAPEX+replacement+O&M cost ($)	0	1064278	527051
Energy supplied from grid in 1st year (kWh)	992952	318458	443892
Utility energy cost before tax in 1st year ($)	74050	20817	31145
Utility demand cost before tax in 1st year ($)	79692	26521	46469
Utility fixed cost before tax in 1st year ($)	5551	5551	5551
Utility minimum cost before tax in 1st year ($)	0	0	0
Utility energy cost after tax ($)	709556	199472	298434
Utility demand cost after tax ($)	763618	254129	445269
Utility fixed cost after tax ($)	53191	53191	53191
Utility minimum cost after tax ($)	0	0	0
Initial cost after tax before incentives ($)		1145520	745458
Initial cost after tax after incentives ($)		720625	444183
O&M and replacement cost after tax ($)		205124	76873
Total life cycle cost after tax ($)	1526366	1365948	1323944
Net present value after tax ($)	0	160418	211011

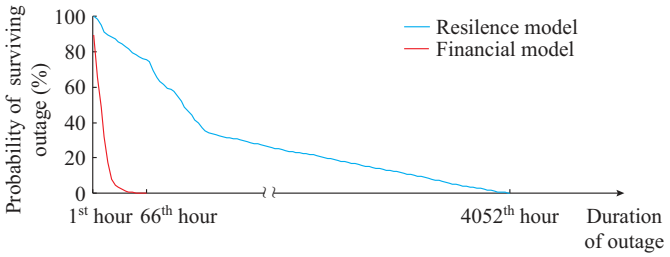

Fig. 6. Probability of surviving outages.

C. With DR

Figure 7 demonstrates the change in load profile before and after the implementation of DR program. It is observed that the peak electricity consumption is reduced by 26.6% which has significant economical, technical, and environmental benefits.

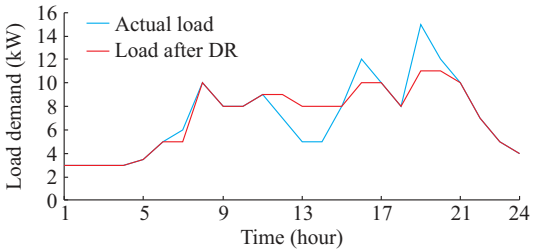

Fig. 7. Load profile with and without DR program.

The details of microgrid system configurations are given in Tables IX and X with DR.

TABLE IX
SIMULATION RESULTS FOR VARIOUS CONFIGURATIONS WITH DR CONFIGURATION

Configuration	PV (kW)	WT (kW)	No. of BESS	DG (kW)	Converter (kW)
PV+WT+BESS+DG	25	10	23	4	12.80
PV+DG+BESS	18		113	5	12.30
WT+DG+BESS		20	29	7	9.65
PV+WT+BESS	40	10	36		16.70
PV+BESS	43		19		21.00
WT+BESS		200	379		30.20

TABLE X
COST ANALYSIS OF FOR VARIOUS CONFIGURATIONS WITH DR

Configuration	NPC ($)	COE ($/kWh)	Operation cost ($)
PV+WT+BESS+DG	193898.70	0.24180	10575.88
PV+DG+BESS	255261.20	0.31820	14524.15
WT+DG+BESS	347733.30	0.43360	22962.22
PV+WT+BESS	94671.38	0.11800	1433.77
PV+BESS	75416.50	0.09402	1110.23
WT+BESS	583289.70	0.72720	9903.33

The SOC of battery throughout the year of PV+WT+DG+BESS configuration is shown in Fig. 8.

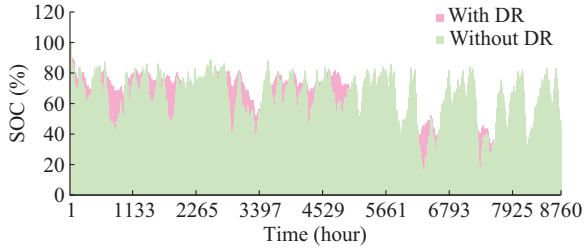

Fig. 8. Hourly SOC of PV+DG+WT+BESS configuration.

Different configurations of hybrid system are simulated considering 100%, 67% and 50% renewable fractions, respectively. After the implementation of DR program, the annual energy production details of each configuration are given in Table XI.

TABLE XI
ANNUAL ENERGY PRODUCTION FOR VARIOUS CONFIGURATIONS WITH DR

Configuration	Source	Annual energy production (kWh/year)	Fraction (%)
PV+WT+DG+BESS	PV	44588	62.70
	WT	2865	4.03
	DG	23653	33.30
PV+DG+BESS	PV	32062	50.60
	DG	31358	49.40
WT+DG+BESS	WT	5731	8.76
	DG	59683	91.20
PV+WT+BESS	PV	71408	95.90
	WT	3072	4.12
PV+BESS	PV	76759	100.00
WT+BESS	WT	57309	100.00

The total annual load consumption of the system is 62050 kWh/year which is met by PV power production 44588 kWh/year, DG power production 23653 kWh/year and WT power production 2865 kWh/year in PV+WT+DG+BESS configuration. It is evident from simulation results that the total electricity demand is supplied by 66.7% renewable fraction and 33.3% non-renewable fraction, respectively. As specified in Table IX, the PV+WT+DG+BESS configuration consists of 25 kW PV, 10 kW WT, 4 kW DG set, 23 battery strings and 12.8 kW converter. As mentioned in Table X, the levelized COE is low for PV+BESS configuration and high for WT+BESS configuration. The annual NPC is low for PV+BESS configuration and high for WT+BESS. The COEs of the hybrid power system are 0.09402 $/kWh, 0.2418 $/kWh, and 0.3182 $/kWh with 100%, 67%, and 50% renewable fractions, respectively. The NPCs of the hybrid power system are $75416, $193898.7, and $255261.2 with 100%, 67%, and 50% renewable fractions, respectively. With the implementation of DR program, NPC and COE are decreased by 24.1% for PV+BESS configuration. The payback periods of PV+WT+DG+BESS, PV+DG+BESS, WT+DG+BESS, PV+WT+BESS, PV+BESS configurations are 0.33 year, 0.43 year, 0.59 year, 0.16 year and 0.12 year, respectively, compared with WT+BESS configuration.

VI. CONCLUSION

This paper evaluates the techno-economic benefits of standalone microgrids with hybrid energy sources and battery energy storage devices. Different feasible configurations of hybrid power system with PV/WT/DG/BESS are studied and a detailed comparative analysis is presented. The capital cost, operation cost, fuel cost, COE and total cost are determined for each configuration. The objective function considered in this paper is the minimization of COE and NPC subject to the reliability index LPSP, zero unmet energy demand, operation reserve and emission reduction. The analysis has been carried out considering the seasonal load variation throughout the year and the renewable fraction of 100%, 65% and 50%, respectively. Also, the load uncertainty is considered in the simulation study. Among the various feasible configurations at the project location, PV+BESS is the most economical with lower NPC and COE. The fuel cost of DGs has significant impact on NPC and COE. The greenhouse gas emissions from hybrid power system is lower than the conventional grid. The hybrid power system with PV+WT+DG+BESS reduces CO and CO_2 emissions by 68.1% per year as compared with the off-grid microgrid integrated with DG alone. Further, the impact of DR is also demonstrated on optimal energy dispatching and techno-commercial benefits. NPC of hybrid system is low with high share of renewables. With the implementation of DR program, NPC and COE are decreased by 24.1% for PV+BESS. In addition, the reserve power requirement with BESS is also assessed to ensure grid resilience.

This paper is helpful to the microgrid operators for decision making, solid investment planning towards rural electrification, competitive microgrid design with hybrid energy sources and effective energy dispatching strategy development. Further, this study can assist microgrid system engineers during preliminary design phase to estimate the capacity of renewable energy source and the project cost.

REFERENCES

[1] International Energy Agency. (2019, Mar.). World energy outlook 2019. [Online]. Available: www.iea.org/weo
[2] R. K. Rajkumar, V. K. Ramachandaramurthy, B. Yong *et al.*, "Techno-economical optimization of hybrid PV/wind/battery system using Neuro-Fuzzy," *Energy*, vol. 36, no. 8, pp. 5148-5153, Aug. 2011.
[3] J. Senthil-Kumar, R. Charles, D. Srinivasan *et al.*, "Hybrid renewable energy-based distribution system for seasonal load variations," *International Journal of Energy Research*, vol. 42, no. 3, pp. 1066-1087, Oct. 2017.
[4] M. Tavakoli, F. Shokridehaki, M. Marzband *et al.*, "A two stage hierarchical control approach for the optimal energy management in commercial building microgrids based on local wind power and PEVs," *Sustainable Cities and Society*, vol. 41, pp. 332-340, Aug. 2018.
[5] H. Zhang, Y. Li, D. W. Gao *et al.*, "Distributed optimal energy management for energy internet," *IEEE Transactions on Industrial Informatics*, vol. 13, no. 6, pp. 3081-3097, Dec. 2017.
[6] Y. Ji, J. Wang, S. Yan *et al.*, "Optimal microgrid energy management integrating intermittent renewable energy and stochastic load," in *Proceedings of IEEE Advanced Information Technology, Electronic and Automation Control Conference*, Chongqing, China, Dec. 2015, pp. 1-5.
[7] C. Li, X. Ge, Y. Zheng *et al.*, "Techno-economic feasibility study of autonomous hybrid wind/PV/battery power system for a household in Urumqi, China," *Energy*, vol. 55, pp. 263-272, Jun. 2013.
[8] L. Olatomiwa, S. Mekhilef, A. S. N. Huda *et al.*, "Techno-economic analysis of hybrid PV-diesel-battery and PV-wind-diesel-battery power

systems for mobile BTS: the way forward for rural development," *Energy Science & Engineering*, vol. 3, no. 4, pp. 271-285, Apr. 2015.
[9] M. A. M. Ramli, A. Hiendro, and Y. A. Al-Turki. "Techno-economic energy analysis of wind/solar hybrid system: case study for western coastal area of Saudi Arabia," *Renewable Energy*, vol. 91, pp. 374-385, Jun. 2016.
[10] W. M. Amutha and V. Rajini, "Cost benefit and technical analysis of rural electrification alternatives in southern India using HOMER," *Renewable & Sustainable Energy Reviews*, vol. 62, pp. 236-246, Sept. 2016.
[11] M. Baneshi and F. Hadianfard, "Techno-economic feasibility of hybrid diesel/PV/wind/battery electricity generation systems for non-residential large electricity consumers under southern Iran climate conditions," *Energy Conversion and Management*, vol. 127, pp. 233-244, Nov. 2016.
[12] A. Al-Sharafi, A. Z. Sahin, T. Ayar *et al*., "Techno-economic analysis and optimization of solar and wind energy systems for power generation and hydrogen production in Saudi Arabia," *Renewable & Sustainable Energy Reviews*, vol. 69, pp. 33-49, Mar. 2017.
[13] D. Akinyele, "Analysis of photovoltaic mini-grid systems for remote locations: a techno-economic approach," *International Journal of Energy Research*, vol. 42, no. 3, pp. 1363-1380, Mar. 2018.
[14] A. C. Duman and O. Güler, "Techno-economic analysis of off-grid PV/wind/fuel cell hybrid system combinations with a comparison of regularly and seasonally occupied households," *Sustainable Cities and Society*, vol. 42, pp. 107-126, Oct. 2018.
[15] J. Weber, D. W. Gao, and T. Gao, "Affordable mobile hybrid integrated renewable energy system power plant optimized using HOMER Pro," in *Proceedings of IEEE 2016 North American Power Symposium (NAPS)*, Denver, USA, Sept. 2016, pp. 1-6.
[16] S. Singh, D. W. Gao, and J. Giraldez, "Cost analysis of renewable energy-based microgrids," in *Proceedings of North American Power Symposium (NAPS)*, Morgantown, USA, Sept. 2017, pp. 1-4.
[17] O. Krishan and S. Suhag, "Techno-economic analysis of a hybrid renewable energy system for an energy poor rural community," *Journal of Energy Storage*, vol. 23, pp. 305-319, Jun. 2019.
[18] A. Al-Sharafi, A. Z. Sahin, T. Ayar *et al*., "Techno-economic analysis and optimization of solar and wind energy systems for power generation and hydrogen production in Saudi Arabia," *Renewable and Sustainable Energy Reviews*, vol. 69, pp. 33-49, Mar. 2017.
[19] M. A. P. Mahmud, N. Huda, S. H. Farjana *et al*., "Techno-economic operation and environmental life-cycle assessment of a solar PV-driven islanded microgrid," *IEEE Access*, vol. 7, pp. 111828-111839, Jul. 2019.
[20] N. Nguyen-Hong, H. Nguyen-Duc, and Y. Nakanishi, "Optimal sizing of energy storage devices in isolated wind-diesel systems considering load growth uncertainty," *IEEE Transactions on Industry Applications*, vol. 54, no. 3, pp. 1983-1991, Feb. 2018.
[21] U. Akram, M. Khalid, and S. Shafiq, "Optimal sizing of a wind/solar/battery hybrid grid-connected microgrid system," *IET Renewable Power Generation*, vol. 12, no. 1, pp. 72-80, Jan. 2018.
[22] Y. Zhang, J. Wang, A. Berizzi *et al*., "Life cycle planning of battery energy storage system in off-grid wind-solar-diesel microgrid," *IET Renewable Power Generation*, vol. 12, no. 20, pp. 4451-4461, Nov. 2018.
[23] R. Kaur, V. Krishnasamy, and N. K. Kandasamy, "Optimal sizing of wind-PV-based DC microgrid for telecom power supply in remote areas," *IET Renewable Power Generation*, vol. 12, no. 7, pp. 859-866, May 2018.
[24] M. Combe, A. Mahmoudi, M. H. Haque *et al.*, "Cost effective sizing of an AC mini-grid hybrid power system for a remote area in south Australia," *IET Generation, Transmission & Distribution*, vol. 13, no. 2, pp. 277-287, Jan. 2019.
[25] S. Bandyopadhyay, G. R. C. Mouli, Z. Qin *et al*., "Techno-economical model based optimal sizing of PV-battery systems for microgrids," *IEEE Transactions on Sustainable Energy*, vol. 11, no. 3, pp. 1657-1668, Aug. 2019.
[26] M. Ahmadi, M. E. Lotfy, R. Shigenobu *et al*., "Optimal sizing of multiple renewable energy resources and PV inverter reactive power control encompassing environmental, technical, and economic issues," *IEEE Systems Journal*, vol. 13, no. 3, pp. 3026-3037, Sept. 2019.
[27] M. Khalid, "Wind power economic dispatch – impact of radial basis functional networks and battery energy storage," *IEEE Access*, vol. 7, pp. 36819-36832, Mar. 2019.
[28] A. A. Z. Diab, H. M. Sultan, I. S. Mohamed *et al*., "Application of different optimization algorithms for optimal sizing of PV/wind/diesel/battery storage stand-alone hybrid microgrid," *IEEE Access*, vol. 7, pp. 119223-119245, Aug. 2019.
[29] H. Abniki, S. M. Taghvaei, and S. M. M. Hosseininejad. "Optimal energy management of community microgrids: a risk-based multi-criteria approach," *International Transactions on Electrical Energy Systems*, vol. 28, no. 12, pp. 1-16, Dec. 2018.
[30] I. Alsaidan, W. Gao, and A. Khodaei. "Battery energy storage sizing for commercial customers," in *Proceedings of IEEE PES General Meeting*, Chicago, USA, Jul. 2017, pp. 1-5.
[31] I. Alsaidan, A. Khodaei, and W. Gao. "A comprehensive battery energy storage optimal sizing model for microgrid applications," *IEEE Transactions on Power Systems*, vol. 33, no. 4, pp. 3968-3980, Jul. 2018.
[32] H. Xie, H. Chen, W. Yan *et al*., "Application of energy storage in high penetration renewable energy system," in *Proceedings of IEEE International Conference on Electro Information Technology (EIT)*, Lincoln, USA, Oct. 2017, pp. 188-193.
[33] *Recommendations for Small Renewable Energy and Hybrid Systems for Rural Electrification – Part 4: System Selection and Design*, IEC/TS 62257-4, 2005.
[34] N. D. Hatziargyriou, T. S. Karakatsanis, and M. Papadopoulos, "Probabilistic load flow in distribution systems containing dispersed wind power generation," *IEEE Transactions on Power Systems*, vol. 8, no. 1, pp. 159-165, Feb. 1993.
[35] NREL. (2009, May). HOMER Pro. [Online]. Available: http://www.homerenergy.com.
[36] A. Zakariazadeh, S. Jadid, and P. Siano, "Smart microgrid energy and reserve scheduling with demand response using stochastic optimization," *International Journal of Electrical Power & Energy Systems*, vol. 63, pp. 523-533, Dec. 2014.
[37] N. Venkatesan, J. Solanki, and S. K. Solanki, "Residential demand response model and impact on voltage profile and losses of an electric distribution network," *Applied Energy*, vol. 96, pp. 84-91, Aug. 2012.

Vallem V. V. S. N. Murty received the B.Tech degree in electrical and electronics engineering from Jawaharlal Nehru Technological University, Andhrapradesh, India, in 2010, and the M. Tech degree in power systems from National Institute of Technology (NIT), Kurukshetra, India, in 2013. He is Research Scholar in Department of Electrical Engineering, NIT. He has published 30 research articles in various reputed international journals and conferences. He has received POSOCO Power System Award (PPSA) for best thesis, Tata Rao Award from Institution of Engineers India (IEI) and best research paper awards. His research interests include power systems, distribution system analysis, microgrids, hybrid energy source integration, storage systems, demand response, and reactive power management.

Ashwani Kumar received the B.Tech degree in electrical engineering from Pant Nagar University, Pantnagar, India, in 1988, and the master's degree in power systems from Panjab University, Chandigarh, India, in 1994 with honors. He received the Ph. D. degree from Indian Institute of Technology (IIT), Kanpur, India, in 2003. He did post-doctoral from Tennessee Technological University, Cookeville, USA. He has started collaboration with academic institutions and R&D labs including IIT and Delft University of Technology, Delft, Netherlands for the project work in the area of smart grids. He has executed research projects sponsored by different funding agencies including Department of Science and Technology (DST), All India Council for Technical Education (AICTE), etc. He has also carried out few consultancies assignments for power companies. He has more than 100 publications in international journals. He has guided 11 Ph.D. and more than 45 M. Tech research theses. Eight of his research students have been awarded with prestigious POSOCO Power System Award (PPSA) for best thesis on all India level. He is presently working as Professor in the Department of Electrical Engineering, National Institute of Technology (NIT), Kurukshetra, India. His research interests include power systems, power systems restructuring, transfer capability assessment, congestion management, demand-side management, DG integration, reactive power management, ancillary services, and transmission and distribution pricing.